

## **Integrated geological and seismic site characterization at Priddis, Alberta**

J. Helen Isaac and Don. C. Lawton

### **ABSTRACT**

3C2D and 3D seismic data were acquired during field school in the last few years on and near university lands at Priddis, Alberta. The data were acquired so that we may characterize the shallowest 800 m for the purpose of future experimental CO<sub>2</sub> injection. Sandstones identified on gamma ray logs are assumed to be correlatable with sandstones observed in outcrop in the west of the study area and to strong reflectors seen on the seismic data. Two sands, termed the Middle Paskapoo and Lower Paskapoo, are interpreted to lie at depths of around 440 and 770 m below the surface, respectively, in the centre of the 2010 Priddis 3D survey. The Lower Paskapoo sand is of particular interest as it is under consideration for CO<sub>2</sub> injection. A robust static geological model was developed for the site and several scenarios of CO<sub>2</sub> injection were simulated for cases of low and high reservoir permeability, and assuming a porosity of 8%. At low injection volumes (600 tonnes per year) the maximum free-phase CO<sub>2</sub> plume diameter after 5 years of injection is only 140 m, and updip migration over 100 years of shut is minimal due to solubility, residual and mineral trapping.

### **SEISMIC DATA**

The seismic data interpreted at Priddis consisted of the 2010 and 2007 3D field school surveys and the vertical components of the 2010 and 2009 2D3C field school lines. Processing of the 2010 3D and 2D data is discussed in Isaac and Lawton, 2010 (this volume). Five vintage unmigrated structure stacks were also interpreted to assess the regional structure and to ensure that the interpretation is consistent with that structure. Interpretation of regional structure is not discussed in this paper. All the modern seismic data were loaded into Kingdom Suite for interpretation. Figure 1 shows the location of all the seismic data and significant wells. The 2010 3D survey overlaps, and is slightly larger than, the 2007 3D survey. The processed 2009 2D line does not cover the entire length of the acquired survey because limited offsets of 120-1000 m were input into the stack. Line A-A' on Figure 1 indicates the location of a cross-section created from well logs.

### **GEOLOGY**

The GSC geology maps and geological cross-section (GSC, 1941) show a change in structural style from west to east across the study area. In the west of the study area, the Belly River Formation is exposed at the surface, there are many mapped NNW-SSE trending thrust faults and the surface topography is dominated by linear ridges. The mapped surface dips are to the west and some are very steep. To the east, where the Edmonton Group and Paskapoo Formation outcrop, the topography is gentler, there are fewer faults and the strata dip gently to the east. Cross-section A-A' (Figure 2) created from well logs lies in the east of the study area and shows a relatively undisturbed stratigraphic section below the lower detachment, which is believed to be above the top of the Belly River. The upper detachment is somewhere in the Edmonton Group and

there is a repeat of part of the Edmonton Group between the upper and lower detachments. The shallowest formation present in these wells is the Palaeocene Paskapoo. Identified on these logs are three intervals interpreted to be sandstones from their gamma ray responses and which give strong reflections on the seismic data; we have termed them the Middle Paskapoo A and B sands and the Lower Paskapoo sand. When interpreting the seismic data we made the assumption that the sandstones identified on the logs correlate to the sandstones observed in outcrop.

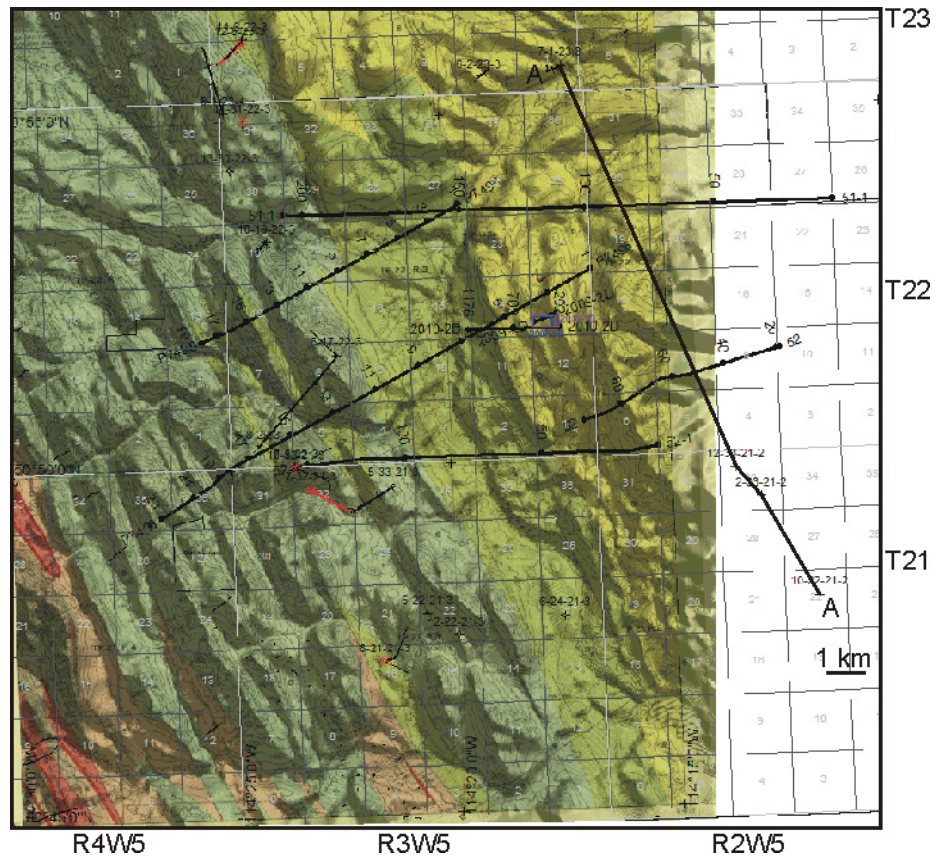


Fig. 1. The location of all the seismic data interpreted in the Priddis area. The 3D surveys are outlined in blue. The map is a composite of the digital elevations and geology.

### SEISMIC DATA INTERPRETATION

The primary data sets used in this interpretation are the 2010 3D and 2010 2D. The 2007 3D survey and 2009 2D line were also interpreted to ensure consistency of seismic reflector identification of all the data.

All the data were referenced to the 2010 3D survey, which has a processing datum of 1260 m. This entailed small static shifts to the other data to tie as best as possible. Figure 3 shows the ties between a line from the 2010 3D survey and the 2010 2D survey with synthetic seismograms for well 12-33-overlain on the section above the Lower Detachment. The synthetic seismograms overlain on each seismic line were generated using wavelets extracted from that line. The lower horizons were also identified by character matching the seismic data with synthetic seismograms and to the regional vintage 2D seismic data. In tying well 12-33-21-2W5 to the seismic data we make the

assumption that the sands identified in the well logs are regionally extensive and correspond to the strong reflections observed in the seismic data.

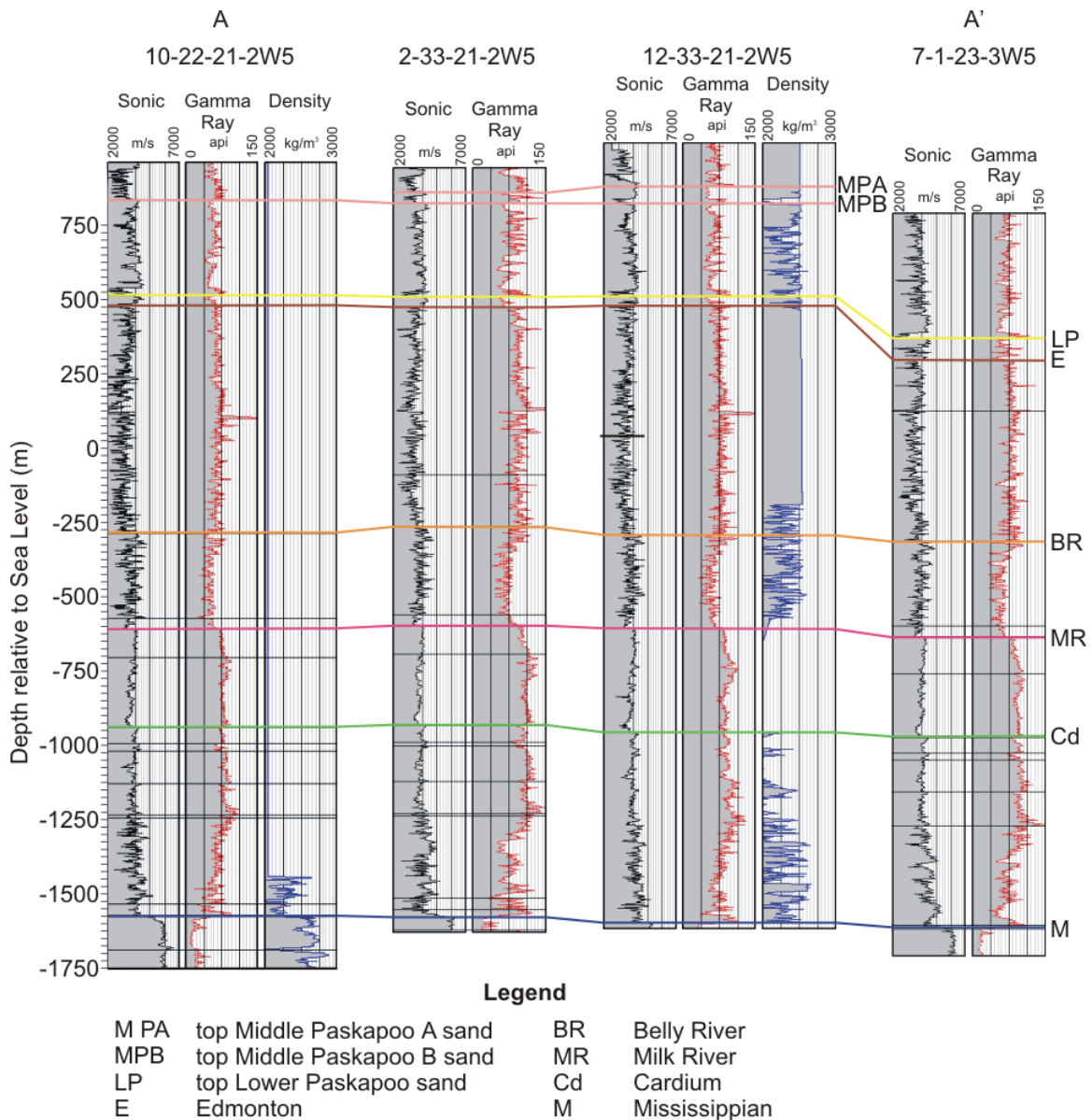


FIG. 2. Well logs showing the correlation of events corresponding to the major seismic reflectors. Sandstones identified on the gamma rays logs are termed Middle Paskapoo A and B and Lower Paskapoo.

We picked reflections for the tops of the Middle Paskapoo A sand, Middle Paskapoo B sand, Lower Paskapoo sand, Edmonton Group, Upper Detachment, Lower Detachment, Belly River, Milk River, Cardium and Mississippian. The Middle Paskapoo and Lower Paskapoo sandstones are best imaged in the west of the 3D surveys. We could not pick the Middle Paskapoo B sand consistently on the 3D data so it is not mapped here. The

interpretation of the Upper and Lower Detachment surfaces are speculative due to the lack of definitive seismic imaging and based on projections from other Foothills seismic data interpretations (Hiebert and Spratt, 1996; MacKay, 1996; Slotboom et al., 1996; Stockmal et al., 1996).

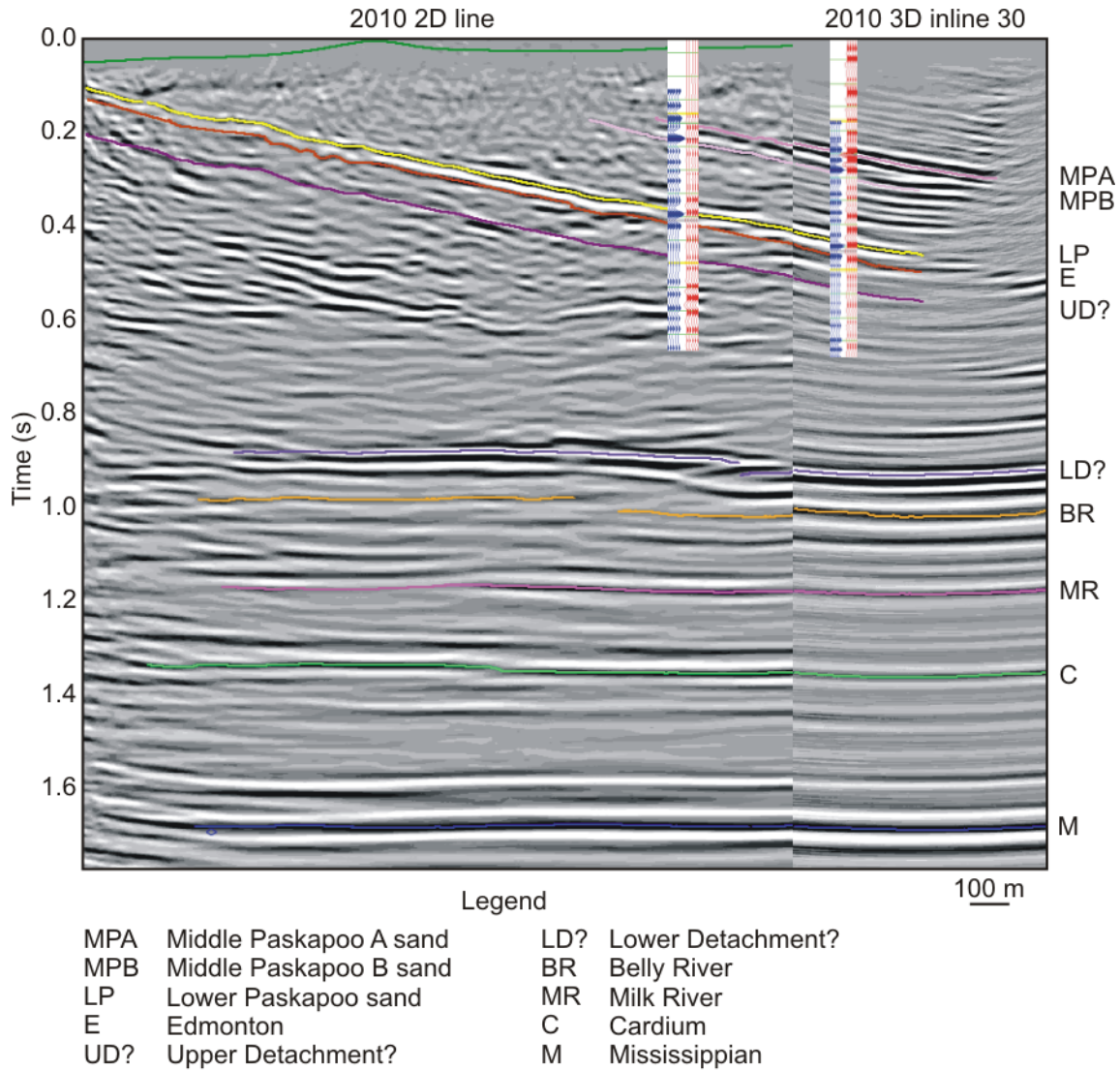


FIG 3. Correlation of the 2010 2D and 3D seismic data with synthetic seismograms. Each synthetic seismogram was created using a wavelet extracted from the appropriate data set.

Figure 4 shows the shallow section above 0.6 s of the 2010 2D line with the interpreted horizons. The data is the bandlimited poststack migration, which shows best the shallowest reflections. The Middle Paskapoo A sand is projected to the surface with a dip of 35°, as mapped by the GSC and measured by us on a recent field trip (Figure 5).



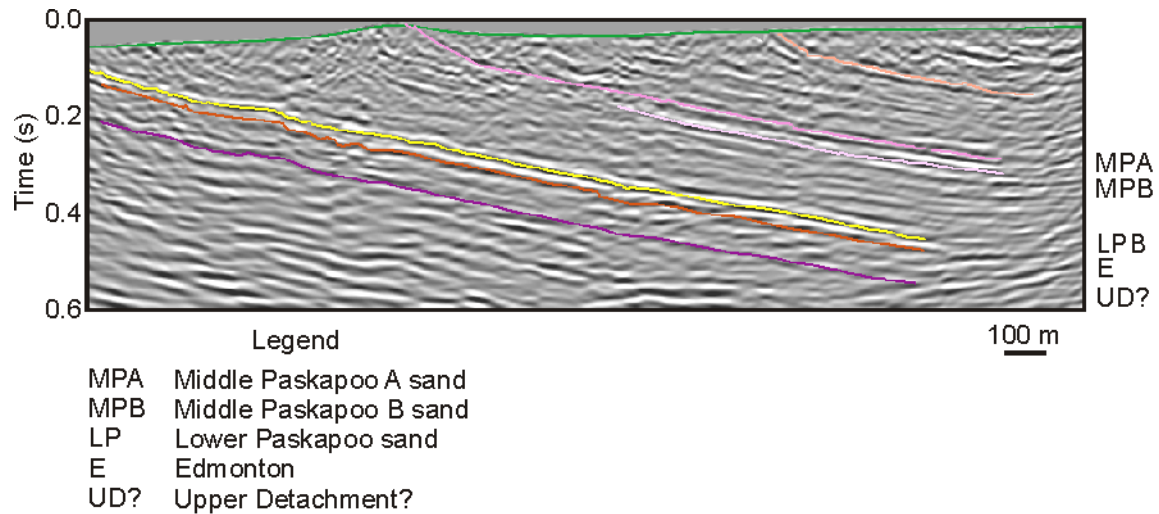


FIG. 4. Interpreted bandlimited poststack migration of the 2010 2D line. The Middle Paskapoo A sand is projected to the surface with the dip measured on outcropping sandstones.

Each horizon was gridded in time and converted to depth. For the depth of the Middle Paskapoo sands we used an average velocity of 3500 m/s, which was derived from the sonic log of well 12-33-21-2W5. For deeper horizons we calculated isochrons and isopachs using interval velocities derived from sonic logs. The depths below the surface of 1245 m at the centre of the 3D survey are estimated to be 470 m for the top Middle Paskapoo A sandstone and 820 m for the top Lower Paskapoo sand.

Figure 8 is a depth cross-section created from the depth grids, displayed at a 1:1 scale. The Lower Paskapoo reflector (yellow) is projected to the surface at a dip angle of  $35^\circ$  to the west of the 2D seismic line.



FIG. 5. Chris Eisinger and Virginia Vera measuring the dip on an outcrop of the sandstone we term Middle Paskapoo A. Ant colonies really like this sandstone.

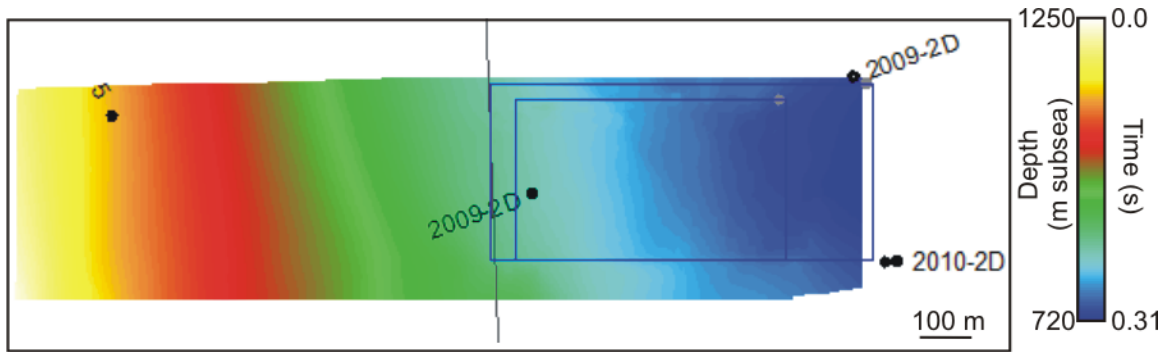


FIG. 6. Map of the Middle Paskapoo A sand.

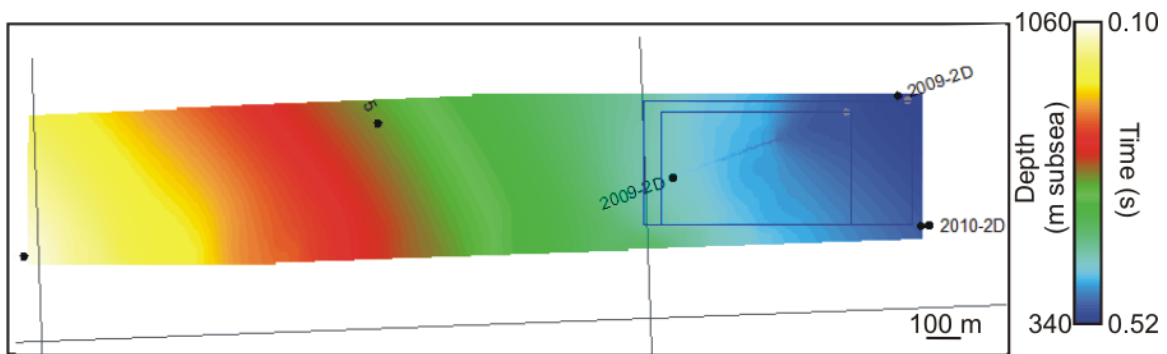


FIG. 7. Map of the Lower Paskapoo sand.

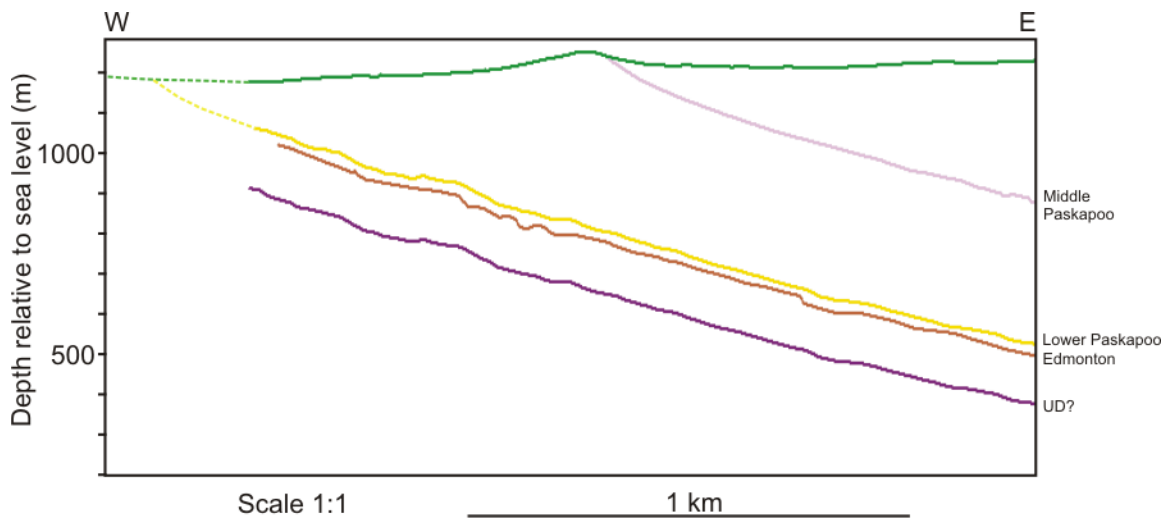


FIG.8. Depth cross-section along the profile of the 2010 2D seismic line, created from depth grids, which were derived from the seismic data interpretation.

### RESERVOIR MODELLING

The site is currently being evaluated for injection and monitoring of small volumes of CO<sub>2</sub> to determine the detection threshold of CO<sub>2</sub> in the shallow to intermediate depth range using seismic and other monitoring methods. The target injection horizon is the

Basal Paskapoo Sandstone and the injection volume is ~600 tonnes per year. In order to predict the behaviour of CO<sub>2</sub> in the basal Paskapoo Formation, a reservoir simulation was undertaken in conjunction with Schlumberger Carbon Services.

A reservoir model was constructed, based on the well data shown in Figure 2 and the interpreted seismic data (Figures 7 and 8). Figure 9 shows the areal extent of the reservoir model developed, including a cross-line from the 3D seismic volume. Initially, the wells were examined to determine porosity of the sandstone horizon of interest, and also the shale cap rock (Figure 10). This analysis showed that the injection zone sandstone has an average porosity of 8%. Permeability was assigned based on a generalized statistical relationship between porosity ( $\theta$ ) and permeability ( $k$ ), courtesy of Schlumberger. Two reservoir models were developed, the first with a permeability of 174 mD and the second with a permeability of 1.74 D; in both cases a ratio of vertical to horizontal permeability ( $K_v/k_h$ ) of 0.3 was assumed.

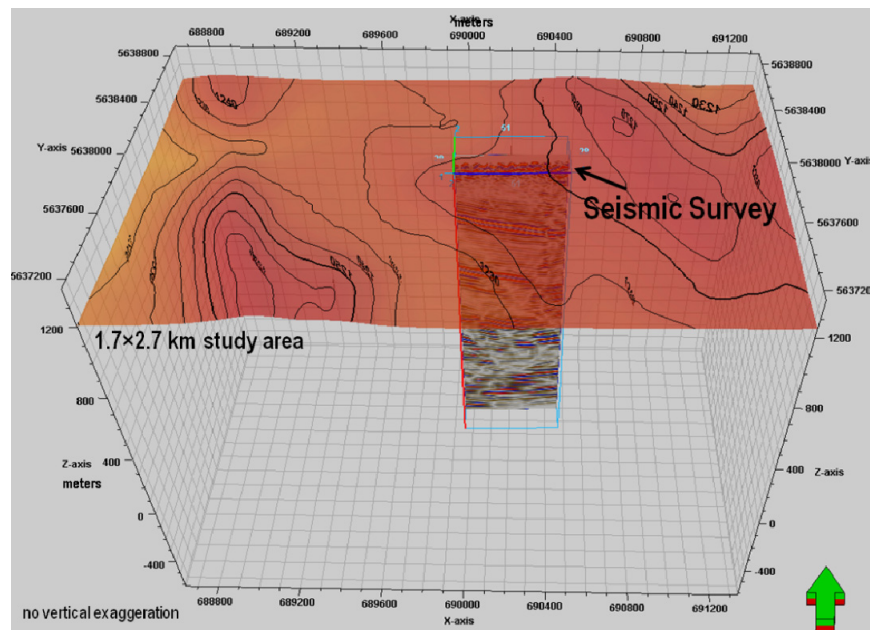


FIG.9. Reservoir model used for the simulation. The extent of the model is 1.7 km x 2.7 km.

The full geological model developed covered of an area of 2.7 x 1.7 km in 269x174 grid blocks (10 m x 10 m grid dimension horizontally). In the vertical direction, the model was constructed from 90 layers representing ~341 m thickness, with variable layers between 1.2 m thick in the injection zone to 30 m thick in the overburden. In order to create some realistic heterogeneity in the model, the 3 wells shown in Figure 10 were imported as pseudowells into the geological model and the properties of individual cells in the model were assigned using a statistical approach. Figure 11 is one realization of the reservoir model with the locations of the pseudowells and the proposed injector and observation well locations shown.



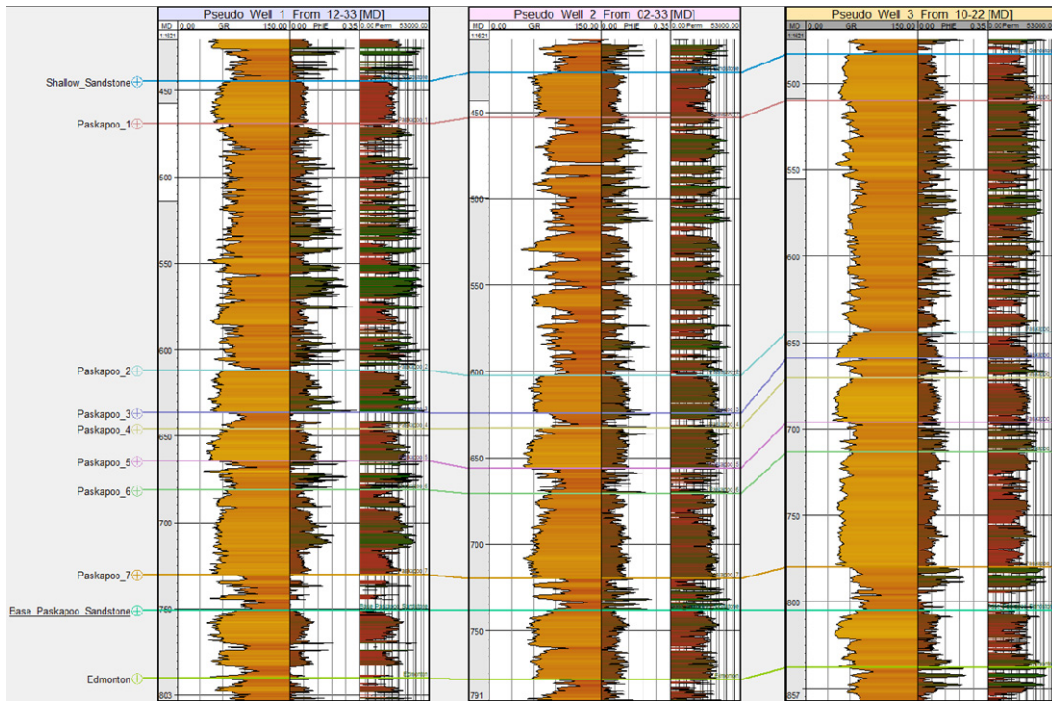


FIG.10. Petrophysical analysis of wells 12-33, 2-33 and 10-32. The proposed injection zone is the Basal Paskapoo Sandstone.

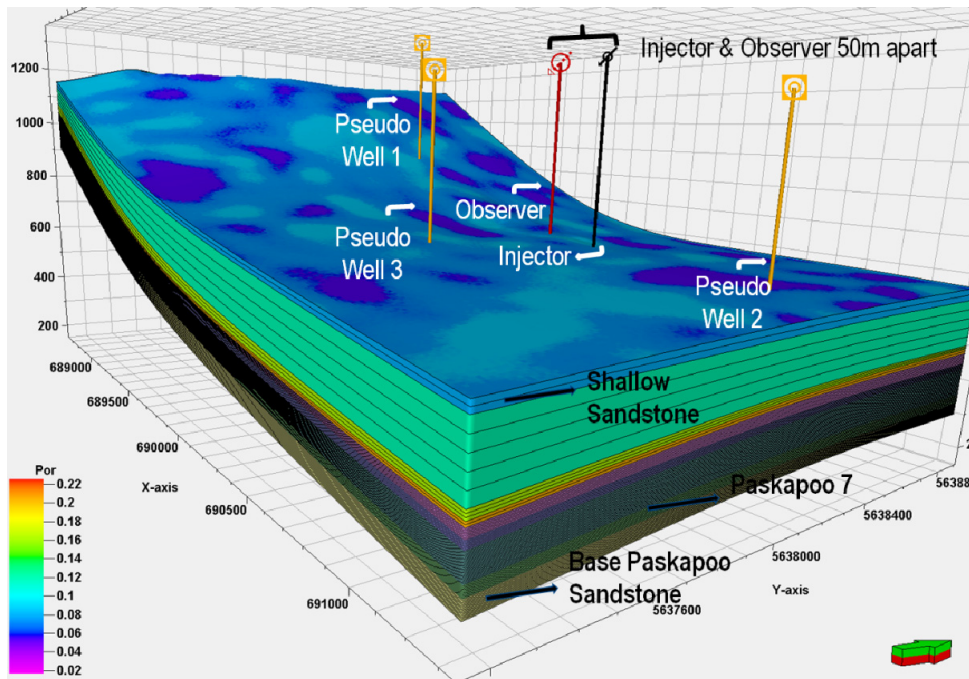


FIG.11. Static geological model showing locations of pseudowells and the injector and observation wells.



The two reservoir realizations, for the low (pessimistic) and high (optimistic) permeability cases, are shown in Figure 12. The changes in permeability between the two models are restricted to the injection horizon which is at the base of the model.

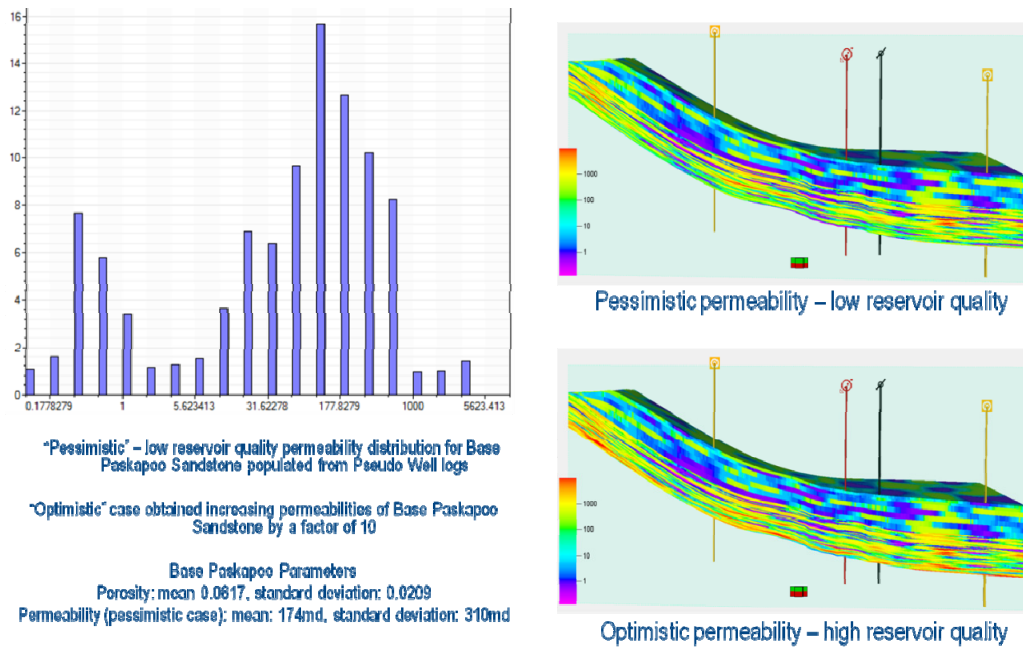


FIG.12. Low (pessimistic) and high (optimistic) permeability reservoir models used for simulations.

Several simulations were run using the models, and the ones reported here are for 5 years of injection at 600 tonnes per year, for both the pessimistic and optimistic reservoir property models. Figures 13 and 14 show respectively the plan view and east-west cross-sectional view of the CO<sub>2</sub> plume at the end of 5 years of injection for the low-permeability model; the plume diameter is about 140 m. After 100 years, the plume saturation profile is shown in Figure 15, with significant dissolution of the CO<sub>2</sub> into the reservoir water and a smaller plume diameter. The residual pressure plume at the site after 100 years shut in is shown in Figure 16; maximum residual pressure is 700 kPa.

Figures 17 through 20 show the same results as Figures 13 to 16 but for higher permeability in the injection horizon. In this case, dissolution of the CO<sub>2</sub> occurs more rapidly than in the low permeability case, and the free-phase CO<sub>2</sub> plume is smaller after 5 years of injection and also after the 100-year shut-in period.

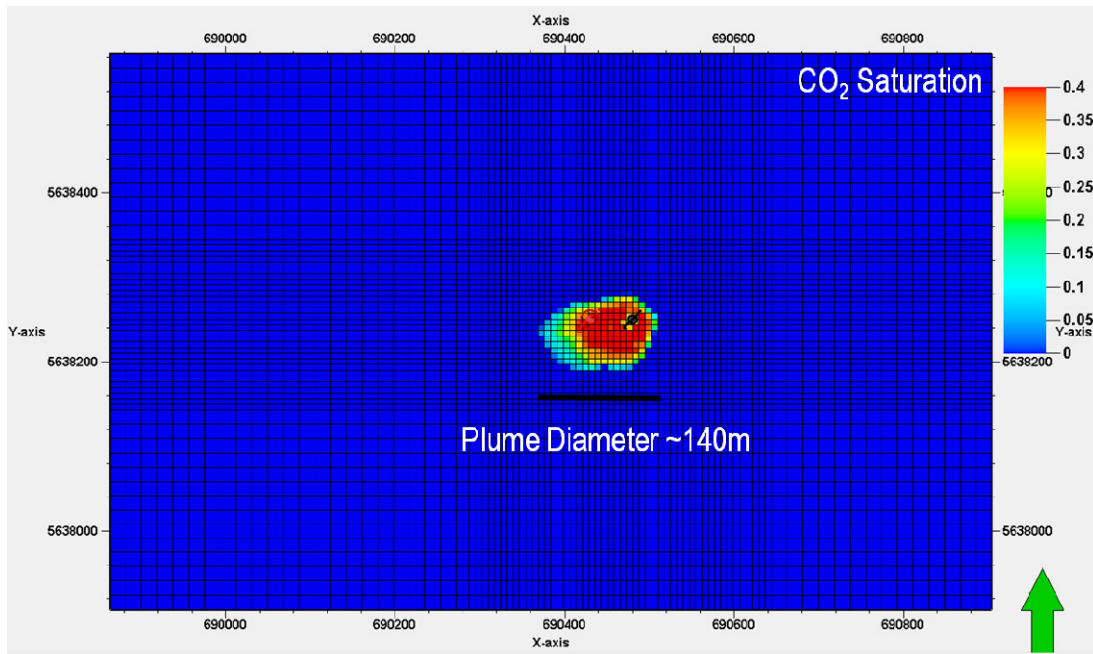


FIG.13. Plan view of CO<sub>2</sub> plume at the 3000 tonnes injected (5 annual injections of 600 tonnes). Low permeability model. Plume diameter is approximately 140 m.

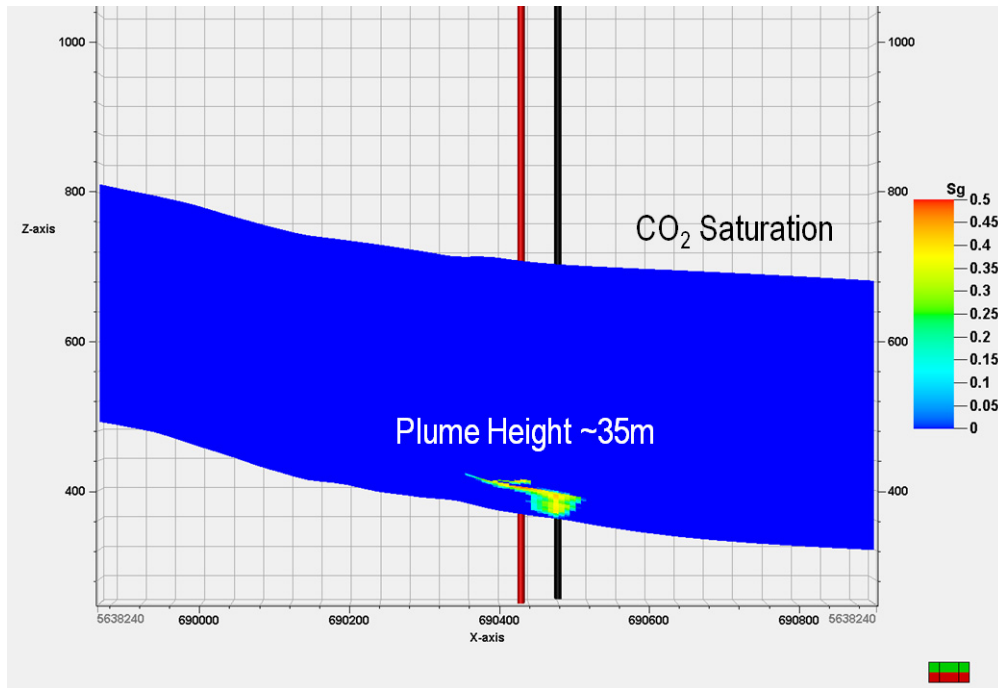


FIG.14. East-west view of CO<sub>2</sub> plume at the 3000 tonnes injected (5 annual injections of 600 tonnes). Low permeability model. Plume diameter is approximately 140 m.

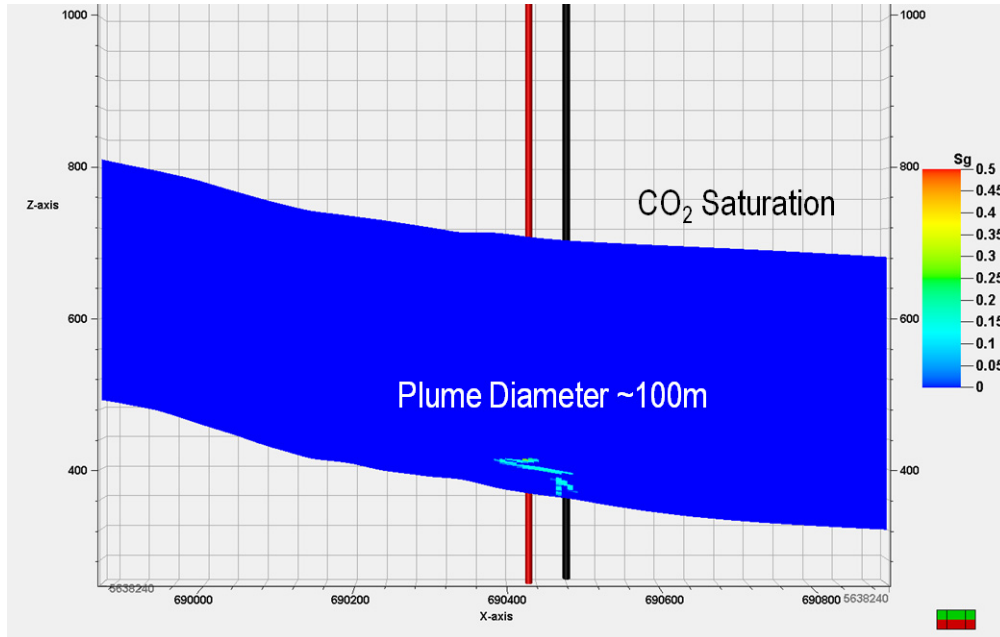


FIG.15. East-west view of CO<sub>2</sub> plume after the 3000 tonnes injected (600 t/y over 5 years) and shut in for 100 years. Low permeability model. Plume diameter is reduced to ~100m due to CO<sub>2</sub> dissolution.

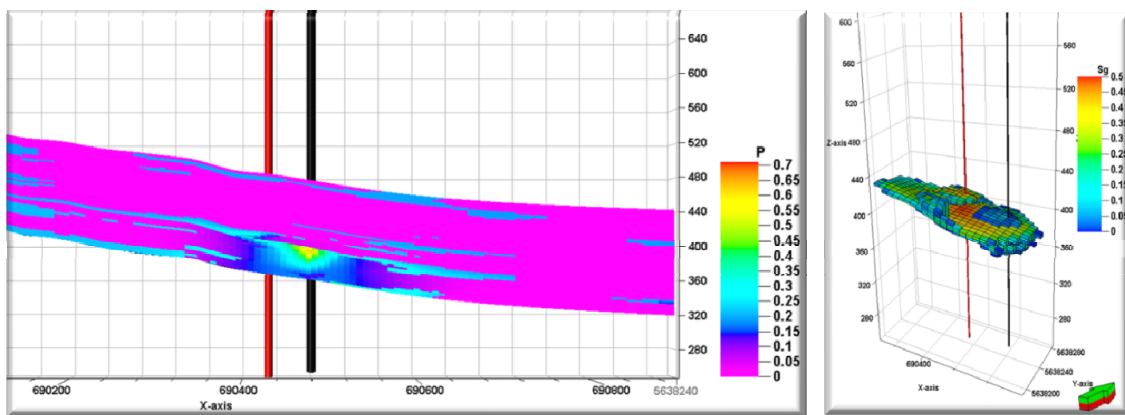


FIG.16. Differential pressure after 3000 tonnes of CO<sub>2</sub> injected (600 t/y over 5 years) and shut in for 100 years; low permeability model

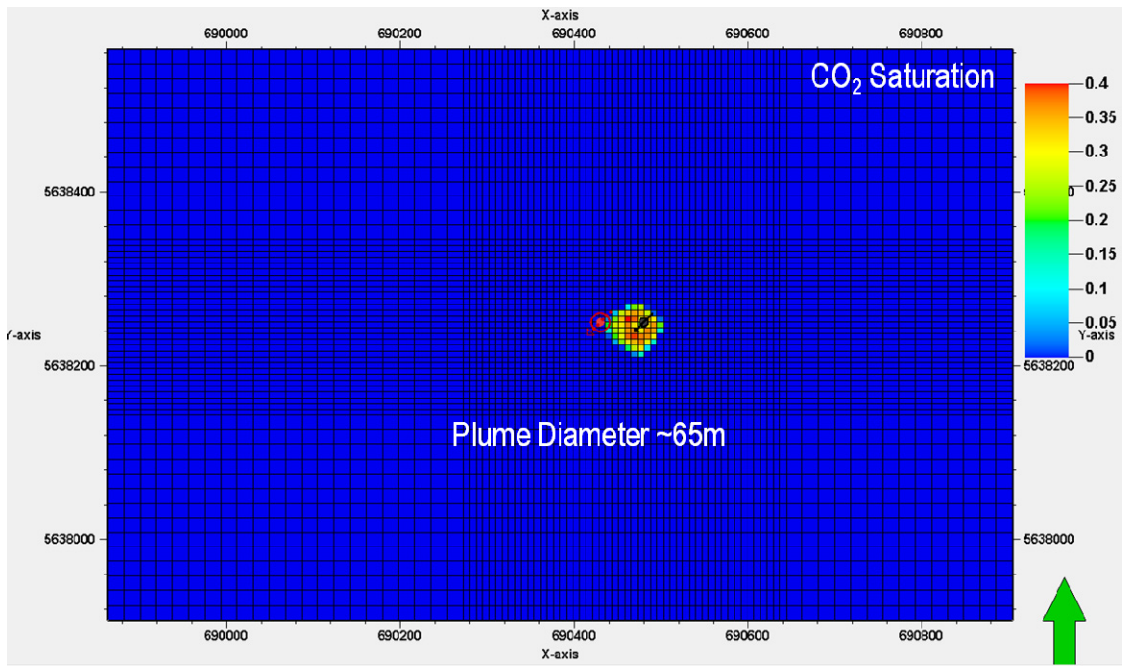


FIG.17. Plan view of CO<sub>2</sub> plume at the 3000 tonnes injected (5 annual injections of 600 tonnes). High permeability model. Thick plume diameter is approximately 65 m.

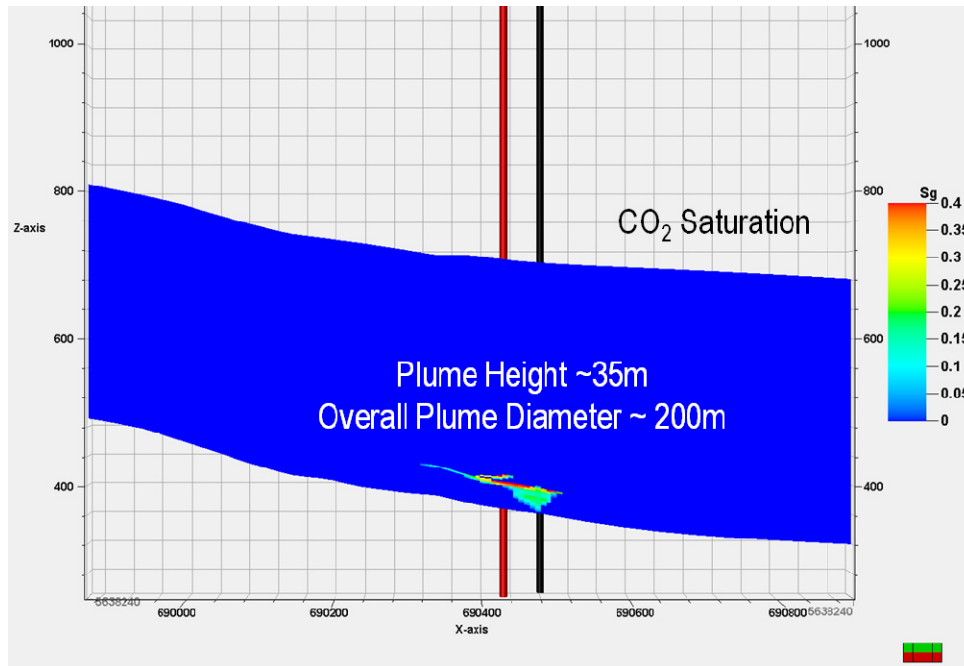


FIG.18. East-west view of CO<sub>2</sub> plume at the 3000 tonnes injected (5 annual injections of 600 tonnes). High permeability model. Thin plume diameter is approximately 200 m.



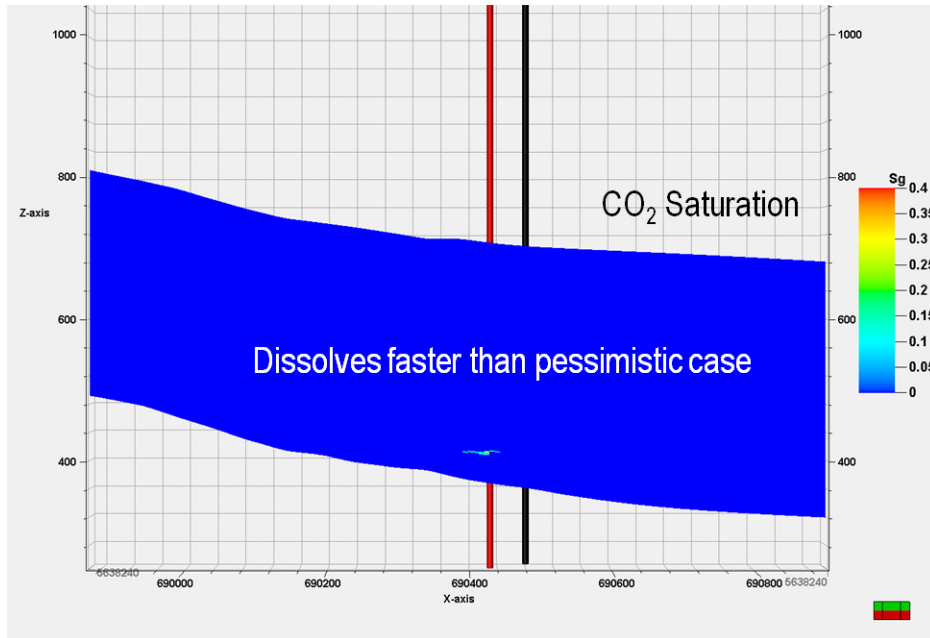


FIG.19. East-west view of CO<sub>2</sub> plume after the 3000 tonnes (600 t/y over 5 years) injected and shut in for 100 years. High permeability model. Greater contact area of CO<sub>2</sub> leads to faster dissolution than in the low permeability case.

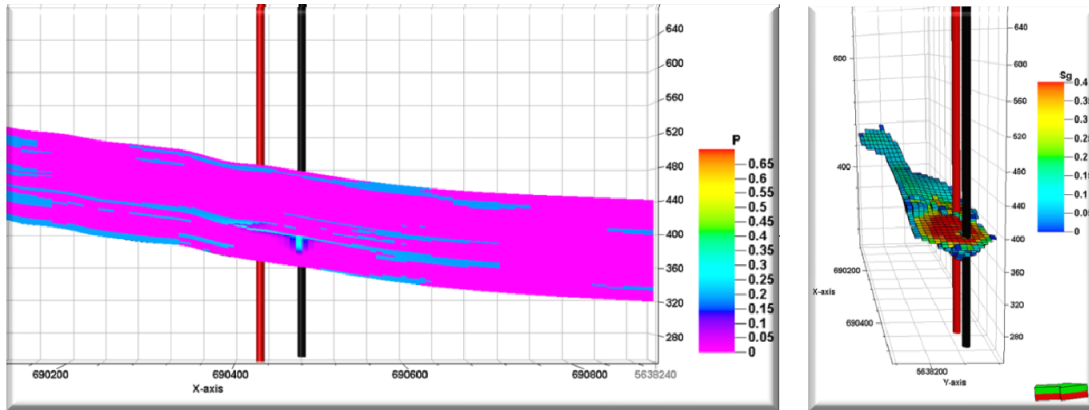


FIG.20. Differential pressure after 3000 tonnes of CO<sub>2</sub> injected (600 t/y over 5 years) and shut in for 100 years; high permeability model. Pressure has dissipated more rapidly than for the low permeability model.

## **SUMMARY**

We interpreted 2D and 3D seismic data acquired at field school near Priddis. Geological and well data were integrated into the interpretation. Bright reflectors observed on the seismic data between 0.2 and 0.5 s are correlated to sandstones picked on gamma ray logs and to outcropping sands. A robust static geological model was developed for the site. Average porosity of the Basal Paskapoo sand was found to be 8% and two models of reservoir permeability were tested – 174 mD and 1.74 D. Several scenarios of CO<sub>2</sub> injection were simulated and the CO<sub>2</sub> plume modelled after 5 years of injection and after a shut-in post-injection period of 100 years. At low injection volumes (600 tonnes per year) the maximum free-phase CO<sub>2</sub> plume diameter after 5 years of injection is only 140 m, and updip migration over 100 years of shut is minimal due to solubility, residual and mineral trapping.

## **ACKNOWLEDGEMENTS**

We would like to thank the faculty, staff and students who worked at field school to acquire the seismic data we interpreted. The CREWES sponsors are thanked for their continued support. We gratefully thank software providers Landmark Graphics (ProMAX), Seismic Micro-Technology, Inc. (Kingdom Suite) and Global Mapper. We also acknowledge reservoir simulation and modelling work undertaken by Schlumberger Carbon Services.

## **REFERENCES**

- Geological Survey of Canada., 1941, Geology and structure cross-sections, Fish Creek, Alberta, Map 667A, scale 1:63,360.
- Hiebert, S. N. and D. A. Spratt, 1996, Geometry of the thrust front near Pincher Creek, Alberta: Bulletin of Canadian Petroleum Geology, Vol. 44, 195-201.
- Isaac, J. H. and D. C. Lawton, 2010, Processing of the 2010 field school 3D and 2D seismic data from Priddis, Alberta, CREWES Research Report, Vol. 22.
- MacKay, P. A., 1996, The Highwood Structure: a tectonic wedge at the foreland edge of the southern Canadian Cordillera: Bulletin of Canadian Petroleum Geology, Vol. 44, 215-232.
- Slotboom, R. T., D. C. Lawton and D.A. Spratt, 1996, Triangle zone at Jumping Pound, Alberta: Bulletin of Canadian Petroleum Geology, Vol. 44, 233-243.
- Stockmal, G. S., P. A. MacKay, D. C. Lawton and D. A. Spratt, 1996, The Oldman River triangle zone: a complicated tectonic wedge delineated by new structural mapping and seismic interpretation: Bulletin of Canadian Petroleum Geology, Vol. 44, 202-214.